

Physical Optics Simulations with PHASE for SwissFEL Beamlines

U. Flechsig*, J. Bahr[†], R. Follath* and S. Reiche*

*Paul Scherrer Institut, Swiss Light Source, 5232 Villigen PSI, Switzerland

[†]Helmholtz Zentrum Berlin, Germany

Abstract. PHASE is a software tool for physical optics simulation based on the stationary phase approximation method. The code is under continuous development since about 20 years and has been used for instance for fundamental studies and ray tracing of various beamlines at the Swiss Light Source. Along with the planning for SwissFEL a new hard X-ray free electron laser under construction, new features have been added to permit practical performance predictions including diffraction effects which emerge with the fully coherent source. We present the application of the package on the example of the ARAMIS 1 beamline at SwissFEL. The X-ray pulse calculated with GENESIS and given as an electrical field distribution has been propagated through the beamline to the sample position. We demonstrate the new features of PHASE like the treatment of measured figure errors, apertures and coatings of the mirrors and the application of Fourier optics propagators for free space propagation.

Keywords: X-rays, beamline optics, synchrotron radiation, XFEL

PACS: 07.85.Qe, 42.79.Dj

INTRODUCTION

The new X-ray sources like free electron lasers (FELs) or diffraction limited storage rings stimulate the development of design tools in the field of X-ray optics. To exploit the unique properties, in particular the transverse coherence and time structure, to predict realistically the parameters of the X-ray pulse at the sample or to find an optimum beamline layout requires physical optics methods. The software package PHASE is one example which has been under continuous development since about 20 years and is now a comprehensive tool box for physical- and geometrical optics calculations. The basic approach of the wave package propagation part is the evaluation of the Fresnel-Kirchhoff integral by means of an analytic expansion of the optical path length around the critical points (CP) which is called stationary phase approximation (SPA). In PHASE a 2nd order phase expansion is implemented which is represented by a complex value characterizing the principle ray and a scaling factor for the analytically integrated contributions around the CP. While the SPA method is intuitively relative easy to understand, the serious mathematical treatment is rather complex [1]. For details about the fundamental principles of PHASE see for instance [2, 3], for a recent summary of PHASE features [4]. There are other beam propagation methods for instance the finite-difference technique [5] or Fourier optics FO implemented for instance in SRW [6] and partly also implemented within PHASE.

In the next sections we present the application of various features of PHASE for the performance prediction of the ARAMIS 1 beamline at SwissFEL. We propagate an electrical field distribution calculated by the 3D FEL simulation code GENESIS [7] through the beamline. The simulation includes realistic figure errors, coatings and should give a quantitative reference for the performance measurements planned during commissioning.

ARAMIS 1 BEAMLINE AT SWISSFEL

The optical layout of the ARAMIS 1 beamline for pump-probe spectroscopy is shown in Fig. 1. Two flat horizontally deflecting and retractable distribution mirrors in sequence deliver the beam into the ARAMIS 1 branch line. It follows a retractable system of double crystal monochromator and higher order rejection mirrors (not considered in the following simulations) and a Kirkpatrick Baez KB type [8] focusing system with two plane elliptical mirrors and 1.5 m working distance. The relevant parameters of the optical elements are given in Table 1. A detailed description of the optical design can be found elsewhere [9].

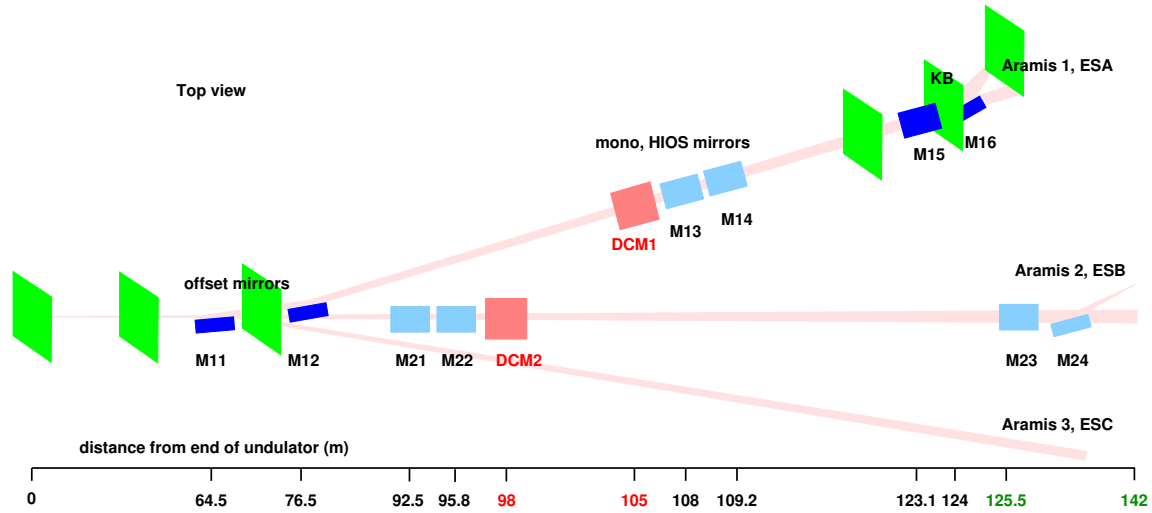


FIGURE 1. Optical layout of the ARAMIS beamlines, mirrors: blue, DCM: red, beam paths: pink, virtual screens: green (see text).

TABLE 1. Selected data of the optical elements.

parameter	M11	M12	M15	M16
shape	flat	flat	plane elliptical	plane elliptical
position (m)	64.5	76.5	123.1	124
opt. surface size (mm ²)	630 × 30	630 × 30	500 × 20	500 × 20
coating	Mo/B ₄ C	Mo/B ₄ C	Mo/B ₄ C	Mo/B ₄ C
source distance (m)	-	-	123.1	124
image distance (m)	-	-	2.4	1.5
grazing angle (mrad)	3	3	4	4
angle to normal (°)	89.8281	89.8281	89.7708	89.7708
direction of deflection	left	left	up	left

SOURCE

The electrical field distribution at the saturation point has been calculated with GENESIS for a photon energy of 12.4 keV and a pulse energy of 0.2 mJ. The intensity and phase distributions are shown in Fig. 2. For the simulations we put the saturation point to the end of the undulator¹.

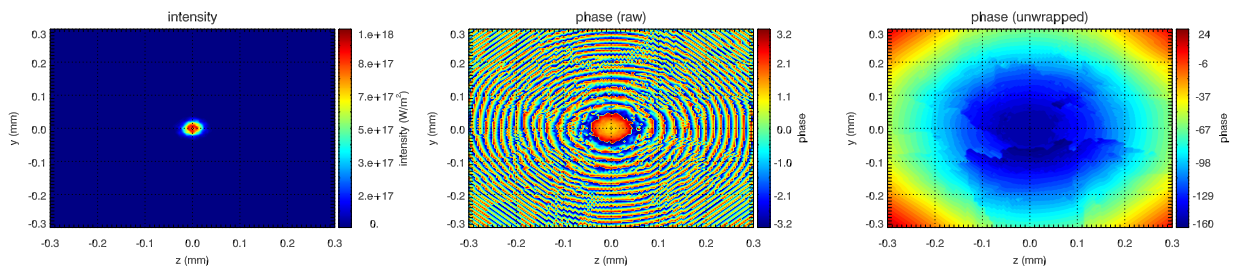


FIGURE 2. Intensity and phase (raw and unwrapped) at the end of the ARAMIS undulator. Calculation with GENESIS, photon energy: 12.4 keV, size FWHM: 33 μ m, power: $W = 1.3$ GW, $W_{max} = 9.5 \times 10^{17}$ W/m², grid: (151 × 151) points, (0.6 × 0.6) mm.

¹ In practice the saturation point is typically within the undulator length. To fulfill our assumption we open/switch off undulator modules upstream.

UNFOCUSED BEAM AT SAMPLE POSITION

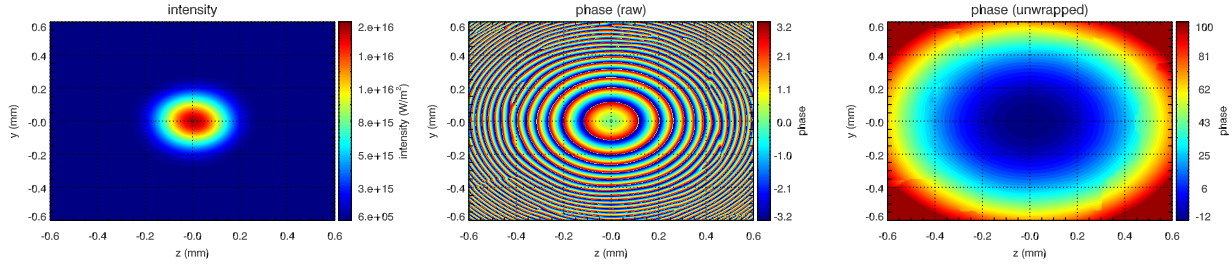


FIGURE 3. Intensity and phase (raw and unwrapped) at the sample position 125.5 m after the undulator, KB retracted. FO propagation, photon energy: 12.4 keV, size FWHM: 250 μm , power $W = 1.1 \text{ GW}$, $W_{\text{max}} = 1.6 \times 10^{16} \text{ W/m}^2$, grid: (729 \times 729) points, $\approx (3 \times 3) \text{ mm}$.

To model an unfocused beam at sample position we assume the flat distribution mirrors are ideal (no figure errors), no beam limiting apertures and the KB retracted. For this purpose a FO propagation with the IDL object included in PHASE is appropriate. We used the following sequence:

```
emf=initphase()           ;; construct object
emf->h5_read, 'aramis1.h5' ;; read genesis file with electrical field
emf->scalefield, 0.95*0.95 ;; scale for reflectivity of 2 mirrors
emf->resize, newsize=729  ;; change grid
emf->propfourier, drift=125.5 ;; propagate
emf->plotintensity       ;; plot etc.
...
```

After constructing our object and reading the electrical field we apply the reflectivity factor to the field. The Mo coating at 12.4 keV has a reflectivity of 0.95², for two mirrors we have $0.95 \times 0.95 \approx 0.9$. Next we do a zero padding and increase the number of points in both directions from 151 (in the file) to 729 ($3^6 = 729$). This is required to limit FFT artifacts, in detail: a) we want to be close to the so called critical sampling condition:

$$\text{wavelength} \times \text{drift} = \frac{\text{width}^2}{\text{number of points}},$$

b) we prefer an odd number of points to have one point in the center and c) the FFT calculates faster if the number of points is a power of small integers {2,3,5}. The critical sampling condition can be checked with the method `emf->checksampling, drift=125.5`. For the propagation we use `propfourier` – a transfer function based propagator ($FFT^{-1} \rightarrow \text{propagation} \rightarrow FFT^{+1}$). Alternatively we could have used `propfresnel` which is slightly faster since it requires just one *FFT* but changes the grid size which we do not want here. For introduction to the FO principles see [10]. Our results are shown in Fig. 3. We expect a spot size of 250 μm FWHM and a intensity maximum of $1.6 \times 10^{16} \text{ W/m}^2$.

² See for instance: http://henke.lbl.gov/optical_constants/mirror2.html

IDEAL AND REAL OPTICS

As a new feature PHASE allows simulations with real optics i.e. the finite size of optical elements, reflectivity, phase shift of coatings, alignment tolerances and figure errors are included. Applying Marechal criterion for a diffraction-limited optics we need mirrors with a figure error in the order of 1 nm rms. Fig. 4 shows a profile measurement of a mirror comparable to our specification which has been used in our simulations for all mirrors. The figure errors must be provided in a hdf5 file, the file may contain errors for multiple elements, 1D or 2D data are accepted, values outside the defined area will be extrapolated from boundary values.

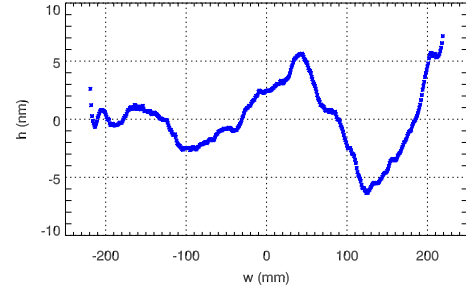


FIGURE 4. Measured height profile of a real mirror, statistics: 2.8 nm, 100 nrad, (both rms). The measured data of a real mirror is courtesy of the LCLS team.

BEAMLINE PERFORMANCE WITH DISTRIBUTION MIRRORS AND KB

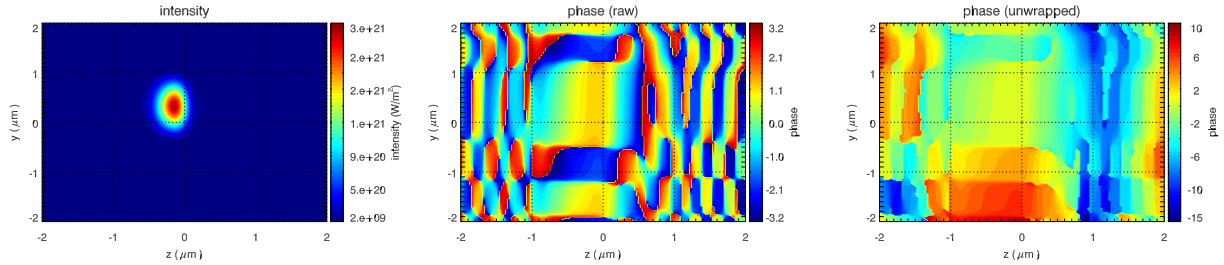


FIGURE 5. Intensity and phase (raw and unwrapped) at the focus position at 125.5 m after the undulator, offset mirrors and KB in place, height errors included. SPA propagation, photon energy: 12.4 keV, size FWHM ($h \times v$): (340 × 690) nm, power $W = 0.76$ GW, $W_{max} = 2.8 \times 10^{21}$ W/m², grid: (151 × 151) points, (4 × 4) μm, intermediate image plane between KB: (5001 × 5001) points, shift due to surface error ($h \times v$): (−0.165 × 0.325) μm.

Physical optics calculation of a complex beamline with PHASE has not been done so far. In this section we introduce the procedure. In principle PHASE can handle a beamline with multiple elements directly. To be able to debug and check intermediate results we chose a step by step propagation with consistency checks at each step. First we divided the beamline into sections with just one optical element separated by artificial interfaces, next we propagate the electrical field distribution from interface to interface. In our case we put the following interfaces: I1 at 36 m (position of front end slit), I2 at 70 m (near the center between M11 and M12), I3 at 121 m (position of a slit upstream the KB) and I4 at 123.55 m (center between KB). In the next step we used the graphical user interface `phaseqt` to create input files for the individual propagations from interface to interface. The propagations themselves have been carried out on a high performance computing cluster with `phasempi` which uses the `openmpi` framework to solve tasks in parallel. For the first propagation from the source to I1 we used the FO propagator similar to the unfocused propagation above. For the other propagation steps we used the SPA propagator, the input/output of the fields has been handled with hdf5 files, the finite size of the optics, direction of reflection, coating reflectivity and figure error has been taken into account. At each step the spatial and angular grid settings have been adjusted³. We kept (151 × 151) points for the spatial grid with one exception: between the KB (I4) we finally increased the grid to (5001 × 5001) points, with less points for instance (1001 × 1001) we observed artifacts like periodic spots etc.. Fig. 5 shows the final focus of the KB with FWHM (340 × 690) nm ($h \times v$) and an intensity maximum of $W_{max} = 2.8 \times 10^{21}$ W/m². The image is slightly off-center caused by the height errors of the KB mirrors. The result has been confirmed in several calculations with different grid sizes.

³ Adjusting the grid is likely the most difficult part for using the physical optics mode of PHASE. We solved the problem by using a) the provided autorange function, b) looking to the output of the density cuts (*PO Simpre* etc.) and c) we did consistency calculations with density cuts while slightly changing the grid size.

settings and is in good agreement with the geometrical optics calculations in the next section and estimations from the magnification ratio. In addition we did physical optics calculations with ellipsoidal mirrors instead of KB. We received similar spot sizes which increases our confidence of having realistic results.

GEOMETRICAL OPTICS

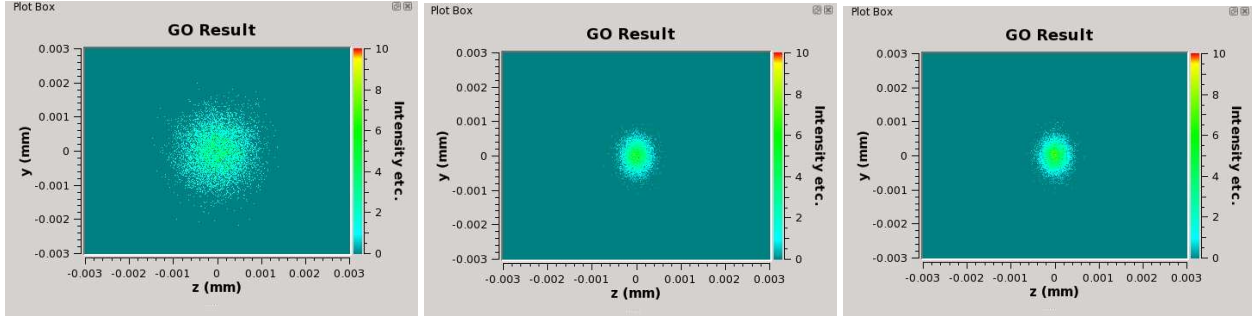


FIGURE 6. Image plane ARAMIS 1 beamline. Ray tracing simulation with different rms slope errors, photon energy: 12.4 keV. left: rms slope error: 20 nrad, FWHM size ($h \times v$): (970 × 1260) nm, center: rms slope error: 2 nrad, FWHM size ($h \times v$): (410 × 650) nm, right: ideal optics – no slope error, FWHM size ($h \times v$): (400 × 640) nm, this is close to theoretical expectation from source size and theoretical demagnification which is (380 × 640) nm.

To confirm the physical optics results we did ray tracing with PHASE . We use an artificial point source with a Gaussian spatial and angular distribution of the rays $\sigma_{y,z} = 14 \mu\text{m}$, $\sigma_{d_y,d_z} = 670 \text{ nrad}$. We did ray tracing assuming different slope errors and for ideal optics. The results are shown on Fig. 6. They confirm the physical optics simulations. The slope errors in the geometrical optics mode of PHASE are assumed to be completely randomly distributed, there is no correlation between the rays, the blur in the image reflects the worst case. Taken this into account we see with 10 nrad rms slope error the optics performs close to the ideal case, with 100 nrad we see a significant broadening.

CONCLUSIONS

The PHASE package is now a powerful physical optics simulation tool for synchrotron and FEL optics. This has been demonstrated with a start to end simulation from the undulator source to the focus on the example of the SwissFEL ARAMIS 1 beamline. For the future the next logic step would be a time resolved simulation, the file structure and tools are ready in principle. We need to distribute the calculations in parallel computing environments and have to work on better bookkeeping and debugging to receive meaningful results. Another development direction is the implementation of crystal optics.

REFERENCES

1. J. Focke, “Asymptotische Entwicklungen mittels der Methode der stationären Phase,” in *Berichte über die Verhandlungen der sächsischen Akademie der Wissenschaften zu Leipzig; Mathematisch Naturwissenschaftliche Klasse*, 101 (3), Sächsische Akademie der Wissenschaften, 1954, pp. 1–48.
2. J. Bahrtdt, *Applied Optics* **34**, 114–127 (1995).
3. J. Bahrtdt, *Phys. Rev. ST Accel. Beams* **10**, 060701 (2007).
4. J. Bahrtdt, U. Flechsig, W. Grizolli, and F. Siewert, *Proc. SPIE* **9209**, 920908–920908–18 (2014).
5. R. Scarmozzino, and R. M. Osgood, *J. Opt. Soc. Am. A* **8**, 724–731 (1991).
6. O. Chubar, M.-E. Couprie, M. Labat, G. Lambert, F. Polack, and O. Tcherbakoff, *Nuclear Instruments and Methods A* **593**, 30–34 (2008).
7. S. Reiche, *Nuclear Instruments and Methods A* **429**, 243 – 248 (1999).
8. P. Kirkpatrick, and A. V. Baez, *J. Opt. Soc. Am.* **38**, 774–776 (1948).
9. R. Follath, U. Flechsig, L. Patthey, and R. Abela, Optical layout of Aramis beamlines, TDR, Technical Design Report FEL-TDR-ARAMIS, PSI (2014).
10. J. W. Goodman, *Introduction to Fourier Optics*, McGraw-Hill, San Francisco, 1968.